DOI: 10.1002/ejoc.200900874

BODIPY-Tetrazine Multichromophoric Derivatives

Cécile Dumas-Verdes,[a] Fabien Miomandre,*[a] Eve Lépicier,[a] Olivier Galangau,[a] Thanh Truc Vu,[a] Gilles Clavier,[a] Rachel Méallet-Renault,[a] and Pierre Audebert*[a]

Keywords: Heterocycles / Dyes/Pigments / Fluorescence / Electrochemistry / Density functional calculations / Chromophores

New dyes based on BODIPY and tetrazine fluorophores connected through a phenyl spacer have been synthesized and their absorption, emission and electrochemical properties characterized. BODIPY can be reversibly oxidized into a stable cation radical whereas tetrazine can be reduced to a stable anion radical. The electrochemical and absorption studies demonstrate that both fluorophores behave independently. The bichromophoric compounds show an expected very weak emission by the BODIPY core that is quenched by the phenoxytetrazine mainly through energy transfer. DFT calculations and spectroelectrochemistry experiments demonstrate that photoinduced electron transfer and energy transfer remain possible when the tetrazine moiety is reduced electrochemically, which prevents switching on of the fluorescence of the BODIPY unit.

Introduction

The search for new fluorescent multichromophoric systems attracts much attention because of their potential applications in various domains such as light-harvesting,[1] sensors[2] or solar concentrators.[3] One area of interest is the possibility of controlling the fluorescence output by an external stimulus such as light, electrical potential or chemicals (proton, metals, etc.). A recent emerging trend is to control the luminescence through the redox state of the system. Several examples of molecular probes based on the redox modification of a moiety attached to the fluorophore have been reported.[4] The principle is based on the modulation of photoinduced electron transfer (PET) from or to the fluorophore. This PET is possible with one state of the sidegroup and is cancelled after its redox modification and it has been reported to be especially sensitive to the linker length and solvent polarity among other factors.[5] Such approaches are applicable in areas such as molecular switches or in the detection of redox-active compounds (e.g., peroxides, NO_x or metals). In addition, we recently demonstrated that the fluorescence of tetrazines (TZs) could also be electrochemically switched on and off in a reversible way.[6] TZ derivatives are presently developed in our laboratory especially for their long-lifetime emission properties associated with their high electron affinity giving rise to a very stable anion radical that is not fluorescent.[7] However, the absorption coefficient of TZ is rather low. Among other possible candidates as redox-switchable fluorophores, BODIPY (4-difluoro-4-bora-3a,4a-diaza-*s*-indacene) derivatives are interesting because of their very good spectroscopic properties, namely strong UV/Vis absorption and quite sharp fluorescence bands with high quantum yields ($\Phi_f > 0.7$). They are also relatively insensitive to the polarity and pH of their environment and small modifications of their structures enable tuning of their fluorescence features.[8] Their synthesis is relatively straightforward starting from pyrrole heterocycles and they can be post-modified at various positions even though the synthesis and photophysical properties of the fully unsubstituted BODIPY core has been reported only very recently.[9] Consequently, these dyes are widely used to label proteins[10] and DNA.[11] Other applications use BODIPY dyes as fluorescent switches,[12] chemosensors,[13] laser dyes[14] and solar cell concentrators.[15] BODIPY is also interestingly used in dyads[16] and multichromophoric or oligomeric fluorescent compounds[17] in which the intrinsic properties of BODIPY can be tuned. Cakmak and Akkaya have described some BODIPY oligomers[17b] in which the boradiazaindacene dyes were converted into phenylethynyl-BODIPY oligomers. As the number of repeating units increases, peak absorption and emission wavelengths are shifted to the red end of the visible spectrum. Such oligomers are very bright red-emitting fluorophores. Arbeloa and co-workers designed multichromophoric dyes with borondipyrromethene (BODIPY) and poly-*p*-phenylene (di- and tri-*p*-phenylene) groups in the same molecule.[18] One of the bichromophoric dyes appeared to be sensitive to the environmental acidity/basicity and could be applied as a proton sensor. Thus, the aim of this work was to present new bichromophoric derivatives

[a] Laboratoire PPSM, CNRS UMR8531, Ecole Normale Supérieure de Cachan, PRES UniverSud,
61 Avenue du Président Wilson, 94235 Cachan, France
Fax: +33-1-47402454
E-mail: mioman@ppsm.ens-cachan.fr

Supporting information for this article is available on the WWW under http://dx.doi.org/10.1002/ejoc.200900874.

comprising one or two BODIPY units and one TZ moiety. The absorption wavelengths of TZ compounds are in the same range as those of BODIPY, but have much lower absorption coefficients. Thus, it can be expected that the association of a donor (BODIPY) and an acceptor (TZ) chromophore in the same molecule leads to photoinduced electron transfer, which, in turn, is likely to be modulated by the redox state of each moiety. For this reason we have synthesized various BODIPY-TZ derivatives differing from each other by the nature of the linker and the relative positions of the two chromophores. The photophysical, electrochemical and absorption spectroelectrochemical properties of these new dyes have been investigated and compared with their parent monochromophoric derivatives. Theoretical calculations have also been performed to better understand the spectroscopic and electrochemical features of these new compounds.

Results and Discussion

Synthesis

The BODIPY derivatives were synthesized using a classic one-pot route: condensation of an aldehyde with 2 equiv. of cryptopyrrole followed by oxidation (either with DDQ or chloranil), deprotonation with DIPEA and finally complexation with boron trifluoride to give BODIPYs **1a**, **1b**, **1c** and **2** in overall yields of around 55%.

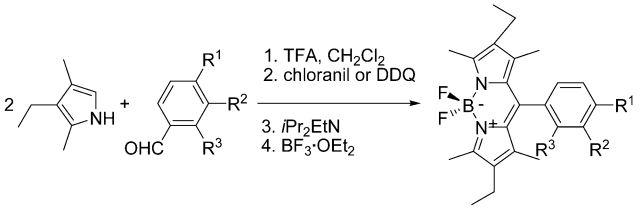

1a: $R^1 = R^3 = H$, $R^2 = OH$
1b: $R^2 = R^3 = H$, $R^1 = OH$
1c: $R^1 = R^2 = H$, $R^3 = OH$
2: $R^1 = OCH_3$, $R^2 = OH$, $R^3 = H$

The main difficulty of this process was to cope with the partial polymerization of pyrrole when using TFA: the controlled addition of this carbonyl activator circumvented this problem. Another issue was the oxidization step using DDQ as we usually isolated the oxidized cleaved compound bearing a hydrogen atom at the C-8 (*meso*) position in large quantities. The use of chloranil was successful in limiting this oxidative cleavage.

The multi-gram synthesis of dichlorotetrazine Cl_2TZ has previously been performed in our laboratory starting from di(pyrazol-1-yl)-*s*-tetrazine.[7,19] The electron-deficient core of Cl_2TZ undergoes nucleophilic substitution with a variety of compounds to give mono- or disubstituted products depending on the nucleophile used. In this work, with the exception of **4c** (due to steric hindrance), the mono-substitution proceeded at atmospheric pressure in the presence of 1 equiv. of 2,4,6-collidine and 1 equiv. of Cl_2TZ with yields of around 36%.

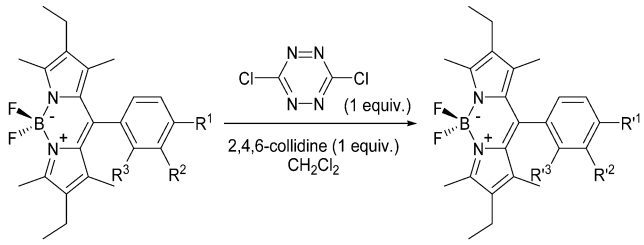

1a: $R^1 = R^3 = H$, $R^2 = OH$
1b: $R^2 = R^3 = H$, $R^1 = OH$
1c: $R^1 = R^2 = H$, $R^3 = OH$
2: $R^1 = OCH_3$, $R^2 = OH$, $R^3 = H$

4a: $R'^1 = R'^3 = H$, $R'^2 = OTzCl$
1b: $R'^2 = R'^3 = H$, $R'^1 = OTzCl$
1c: $R'^1 = R'^2 = H$, $R'^3 = OTzCl$ *
2: $R'^1 = OCH_3$, $R'^2 = OTzCl$, $R'^3 = H$
*sealed tube

The second substitution of Cl_2TZ is usually more difficult as once a chlorine has been substituted by an oxygen, the reactivity of the tetrazine ring decreases due to the electron-donating mesomeric effect of the oxygen atom. Thus, the bichromophoric dyes **5a** and **5b** were synthesized in a sealed tube. The *ortho*-coupled bis-BODIPY compound could not be obtained by this reaction as a result of steric hindrance.

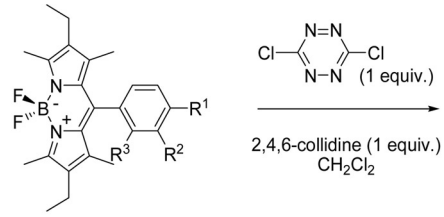

1a: $R^1 = R^3 = H$ $R^2 = OH$
1b: $R^2 = R^3 = H$ $R^1 = OH$

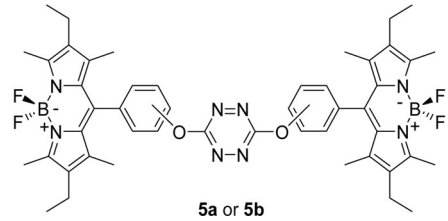

5a or **5b**

Absorption and Emission Spectroscopy

Table 1 shows the spectroscopic features of the various compounds represented in Scheme 1. The BODIPY derivatives **1a**–**c** and **2** display standard spectra for such fluorophores with an intense band in the visible region located at around 525 nm (corresponding to a $\pi \rightarrow \pi^*$ transition) with a vibrational shoulder at a higher energy. A second, less intense band is located in the UV region at around 375 nm. Note that despite the use of different phenols the spectroscopic features of the BODIPY chromophores **1** and **2** are very similar, in agreement with the orthogonal arrangement of the dipyrrin moiety in relation to the phenol ring.

The absorption spectra of the bichromophoric molecules **3** and **4** exhibit a broad maximum in the UV domain corresponding to transitions located both in the tetrazine core and the BODIPY unit. A second maximum located in the visible region is very similar to those observed in the parent

Table 1. Spectroscopic data for the investigated compounds **1**–**5**: absorption wavelengths, absorption coefficients at 530 nm, emission wavelengths and quantum yields.

Compound[a]	λ_{abs} [nm]	ε_{530} [L mol^{-1} cm^{-1}]	λ_{em} [nm][b]	ϕ[c]
1a	378, 526	56000	537	0.80
1b	372, 525	82000	537	0.80
1c	381, 530	83000	544	0.80
2	376, 525	74000	536	0.70
3	375, 528	69000	537	0.05
4a	375, 528	63000	538	0.02
4b	378, 528	78000	538	0.04
4c	384, 533	66000	545	n.d.
5a[d]	377, 523	n.d.	534	n.d.
5b	375, 528	164000	544	0.02

[a] All measurements in dichloromethane. [b] Excitation wavelength: 530 nm. [c] Measured with Rhodamine 590 in methanol as the standard (ϕ_f = 0.83). [d] Determined in acetonitrile.

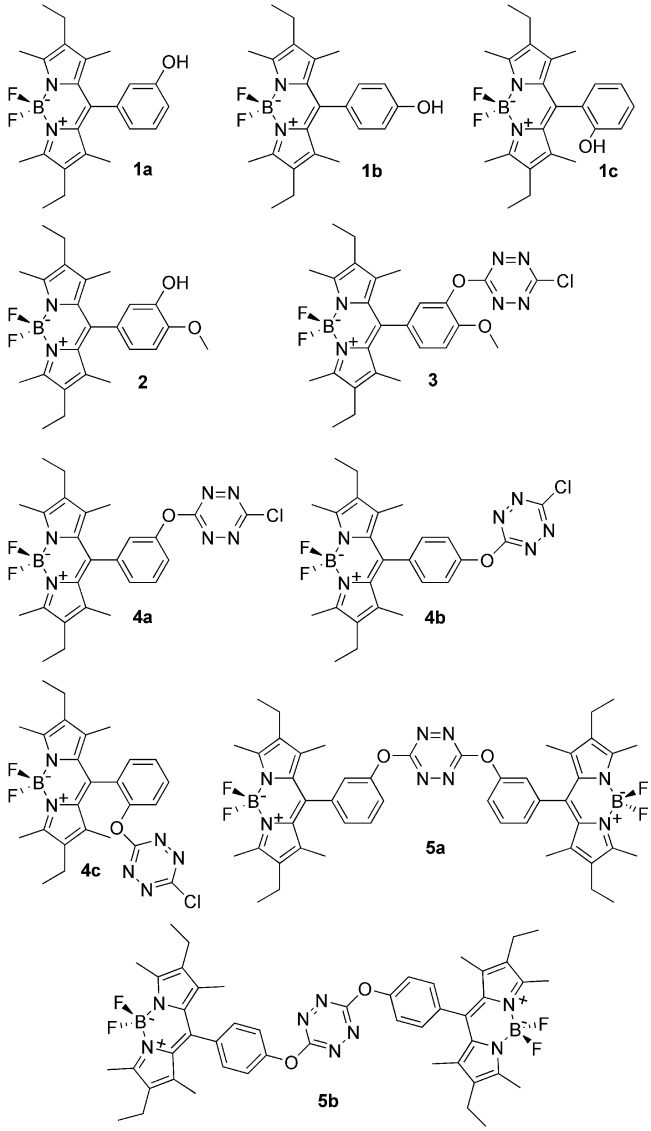

Scheme 1. Structures of the investigated compounds **1**–**5**.

BODIPY compounds **1a**–**c** and **2**. Note that the measured absorption coefficients for this latter transition are in the region of 70000 L mol^{-1} cm^{-1}, in agreement with classical values for BODIPY π→π* transitions. The n→π* transition of the tetrazine core, which lies in the same wavelength range, has a much lower absorption coefficient and is thus hidden underneath that of BODIPY. The spectra of compounds **3** and **4a**–**c** correspond to the sum of their individual components (see Figure 1, A), which demonstrates that no charge transfer state is observed. In the case of compound **5b**, the absorption coefficient for the visible band is nearly twice that of compound **4b**, as expected for a bichromophoric species with two independent chromophores.

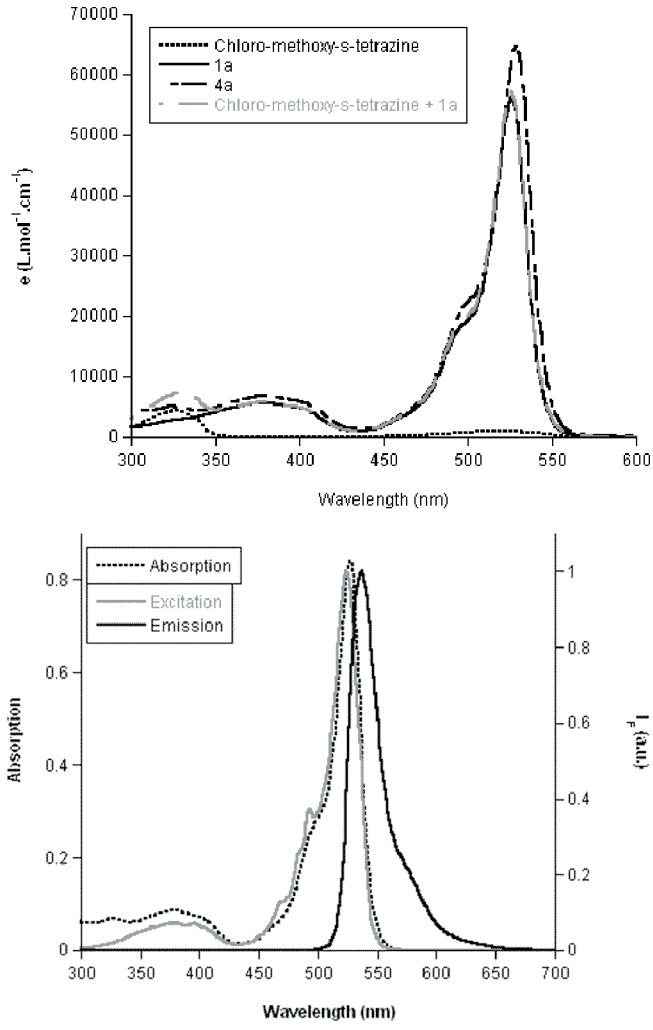

Figure 1. A) Absorption spectra of: chloromethoxy-*s*-tetrazine (from ref.[3]), **1a**, **4a** and chloromethoxy-*s*-tetrazine + **1a**. B) Comparison of the absorption, emission (λ_{exc}) and excitation spectra (λ_{exc}) of **4b**.

Luminescence spectra were recorded in solution (dichloromethane) and display an emission maximum at around 540 nm, which can be ascribed mainly to the BODIPY fluorophore (see Figure 1, B). The luminescence results clearly evidence fluorescence quenching by the tetrazine moiety. Indeed the quantum yield changes from 0.70–0.80 in **1** and **2** (classic value for BODIPY) to 0.02–0.04 for BODIPY-TZ compounds **3** and **4**. This quenching is due to an intramolecular process because no variation in the quantum yield was observed for pure BODIPY in the presence of added

chloromethoxytetrazine. One could expect that the rather strong electron-accepting power of the tetrazine ring would be responsible for the excited-state quenching of the BODIPY moiety through a redox process (see Figure 3). Nevertheless, the quantum yield measured for **4b** in an apolar solvent such as methylcyclohexane is exactly the same as in dichloromethane, which makes the assumption of an energy-transfer mechanism more likely. In addition, excitation spectra (Figure 1, B) as well as monoexponential decays with a lifetime of around 5 ns for **4b** (from time-resolved fluorescence experiments not shown) clearly evidence that the residual luminescence is due to BODIPY and not the chlorophenoxy-TZ moiety.

One could have expected an influence of the position of substitution of the tetrazine on the fluorescence quantum yield. Indeed, other groups have shown such an effect on a BODIPY derivative with a different acceptor, namely maleimide.[20] It appears that in our case the fluorescence quenching is similarly efficient in all cases. Because conjugation is known to be more efficient through *para* rather than *meta* coupling, this result is also in favour of quenching by energy transfer, the similar values for the quantum yields corroborating the fact that the quenching moiety lies at approximately the same distance from the BODIPY core in the *meta*- and *para*-linked compounds (actually calculations show a difference of 15% for the TZ-BODIPY distances in both **4a** and **4b**, which is within the uncertainty for the determination of the quantum yield).

Electrochemistry

A typical cyclovoltammogram for a BODIPY-TZ compound is displayed in Figure 2. Three pairs of peaks can be identified corresponding to the oxidation of BODIPY into its cation radical (near +0.8 V), the reduction of TZ into its anion radical (near –0.75 V) and the reduction of BODIPY into its anion radical (near –1.7 V). The first two peaks are fully reversible as far as concerns the backward versus forward current, although the peak-to-peak separation is greater than 60 mV due to both the uncompensated ohmic drop and sluggish electron transfer, whereas the final peak is only partially reversible, which shows that the anion radical of BODIPY is less stable under these experimental conditions than the tetrazine anion radical.

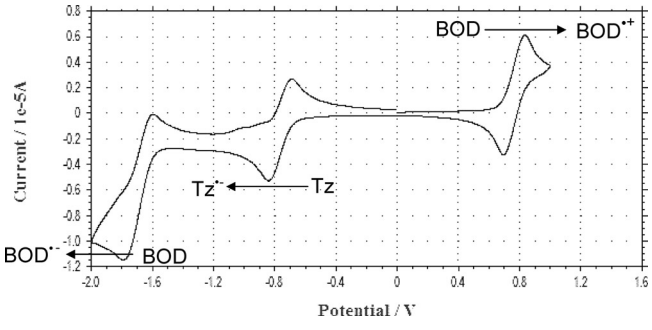

Figure 2. Cyclic voltammetry of compound **4a** in dichloromethane + 0.1 M Bu_4NPF_6. Potentials are referenced to Ag^+ (10^{-2} M)/Ag. Scan rate: 100 mV/s.

The redox potentials for the compounds shown in Scheme 1 are reported in Table 2. A comparison of the data for compounds **4a**–**c** shows that the various standard potentials are almost insensitive to the position of substitution on the phenyl ring, especially those of BODIPY. When comparing the results obtained for BODIPY-TZ compounds **3**–**5** with those for chloromethoxy-*s*-tetrazine ($E°$ = –0.99 V vs. Fc[7]) and for the parent BODIPYs (compounds **1** and **2**), it is clear that the mutual influence of each redox moiety on the standard potential of the other one is weak but more sensitive for the TZ reduction. This means that the apparent conjugation between BODIPY and TZ is not effective in the various bichromophoric compounds, first because the ether linker disrupts the conjugation and secondly because the two subunits are not coplanar (see below for details). The more positive values for the tetrazine reduction potential in the bichromophoric dyes (compared with chloromethoxy-*s*-tetrazine) can be explained by the electron-withdrawing character of the BODIPY-phenyl subunit, as previously observed in BODIPY-ruthenium polypyridine dyes.[16d] This effect is the most sensitive in the case of the *para* linkage in **4b**, whereas for **3** it is partially cancelled by the donor character of the methoxy group on the phenyl ring. In addition, the bis-BODIPY compounds **5a** and **5b** also display unexpectedly high values for the reduction potential of TZ compared with dimethoxy-*s*-TZ tetrazine ($E°$ = –1.25 V vs. Fc[7]): substituting a chlorine by a methoxy group on the TZ core leads to a negative potential shift of about 250 mV, whereas for **5a** and **5b** the shift is much lower (140–170 mV), which confirms that the BODIPY-phenyl unit is much less donating than the methyl group. This is confirmed by the relative positions of the TZ-located LUMOs in compounds **4b** and **5b** compared with the corresponding BODIPY-located HOMOs (see Table 3): the difference between **4b** and **5b** is 0.24 eV, similar to the corresponding difference in the redox potentials (170 mV). The BODIPY reduction is nearly not affected by the TZ subunit, with all the corresponding potentials in the same range except for **1c** in which it is likely a hydrogen bond

Table 2. Electrochemical data for investigated compounds **1**–**5**. Potentials are referenced to Ag^+(0.01 M)/Ag. The reference electrode was checked versus Fc as recommended by IUPAC (between 60 and 90 mV vs. Fc).

Compound[a]	$E°_{ox}$ [V]	$E°_{red1}$ [V]	$E°_{red2}$ [V]
1a	0.73	–	–1.76
1b	0.74	–	–1.70
1c	0.75	–	–1.52
2	0.70	–	–1.70[b]
3	0.75	–0.81	–1.65
4a	0.76	–0.76	–1.70
4b	0.76	–0.71	–1.70[b]
4c	0.73	–0.79	–1.70[b]
5a	0.75	–0.90	–1.63
5b	0.73	–0.88	–1.65

[a] All measurements in dichloromethane + $TBAPF_6$ on Pt, except for **1** which was on Au. [b] Ill-defined because not fully reversible.

Table 3. Energy differences (in eV) between the various frontier orbitals of compounds **3**–**5** and their constitutive fragments.

	$\Delta E_{HOMO–LUMO}$	$\Delta E_{HOMO–LUMO\ (BODIPY)}$	$\Delta E_{HOMO–LUMO\ (TZ)}$	$\Delta E_{HOMO(BODIPY)–HOMO(TZ)}$	$\Delta E_{LUMO(BODIPY)–LUMO(TZ)}$
3	1.93	2.88	3.69	1.76	0.96
4a	1.80	2.88	3.57	1.77	1.08
4b	1.82	2.88	3.55	1.74	1.06
4c	1.88	2.85	3.61	1.72	0.97
5a–**5b**	2.04	2.90	3.52	1.48	0.86

stabilizes the anion radical of BODIPY. Finally, the results of a comparison of the relative current peaks for the TZ reduction with the BODIPY oxidation in **4b** (Figure 2) and **5b** (see the Supporting Information) are in accord with the expected 1:1 and 1:2 exchanged electron ratio, which shows that both moieties maintain their own electroactivity in the bichromophoric compounds.

The electrochemical and spectroscopic data have allowed the relative redox properties of the various neutral, ionic and excited states of both chromophores to be identified. The results are summarized on a redox scale in Figure 3. The oxidation potentials of the anion radical of BODIPY (to the excited BODIPY) and of BODIPY itself (to its cation radical) are found to be close, consistent with the electron being removed from the same orbital. Similarly, the reduction potential of BODIPY (to its anion radical) is close to that of the BODIPY cation radical (to the excited BODIPY) as the electron is added to the same orbital in both cases. The lack of fluorescence of the bichromophoric species could be predicted when one looks at the redox potentials. Indeed, in any case, the absorption of one photon leads to an excited state in which an electron-transfer process from the BODIPY to the TZ ring is thermodynamically favoured. However, in the case of BODIPY fluorescence, which is the main fluorophore in these dyes due to its much higher absorption coefficient, the driving force for PET is only –0.74 eV, which could explain why the quenching mechanism is dominated by energy transfer.

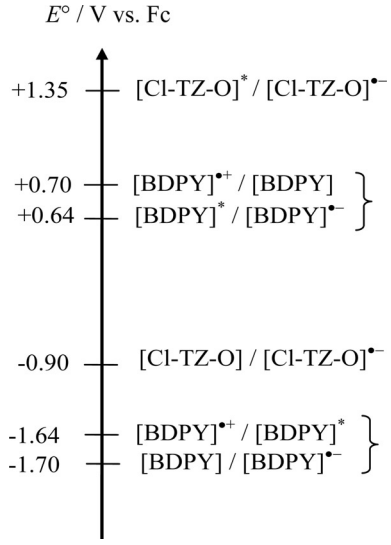

Figure 3. Redox scale for the neutral, ionic and excited-state BODIPY (BDPY) and tetrazine (TZ) couples vs. ferrocene (Fc). The potentials for the couples involving neutral species are average values from Table 2. Those involving excited-state species were calculated from $E_{0–0}$ values extracted from the spectroscopic data.

Theoretical Calculations

Quantum chemical calculations were carried out on bichromophores **3** and **4a**–**c**. Density functional theory (DFT) and time-dependant density functional theory (TD-DFT) calculations at the B3LYP level of theory and with the 6-31+G(d) basis set were performed. For all the bichromophores **3** and **4a**–**c**, the three subunits (BODIPY, phenyl and *s*-tetrazinyloxy) are found to be more are less perpendicular to each other (see Figure 4). This is due to steric hindrance in the case of BODIPY and the phenyl. Indeed, the methyl groups at the 1- and 7-positions of the BODIPY ring force the *meso* substituent (i.e., the phenyl ring) out of the plane of the BODIPY (calculated angle between the planes is between 81 and 87°). On the other hand, the angle between the phenyl and the tetrazinyloxy moieties is a result of the propensity of the oxygen atom to force the two adjacent rings to be nearly perpendicular, but this angle is found to depend on the position of the tetrazinyloxy group on the phenyl. Indeed, in the case of **4b**, the angle is calculated at 87° but decreases to 77° for **4a** and **4c**. This is due to the proximity of the BODIPY ring and its methyl substituents, which causes some steric hindrance. The close proximity of the tetrazine and BODIPY rings is very pronounced in the case of **4c**, as reflected by the loss of symmetry of the two fluorine atoms seen in the ^{19}F NMR spectrum. Indeed a multiplet corresponding to an ABX spin system is observed instead of the usual quartet. The geometry optimization also clearly shows that the tetrazine ring lies on one side of the BODIPY and is approximately 6 Å from one fluorine atom with no possibility of free rotation around the BODIPY ring.

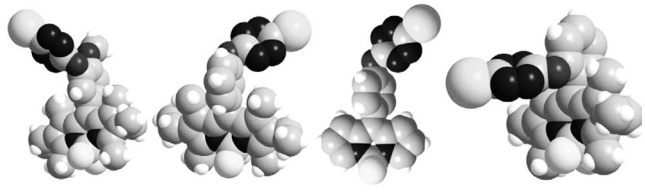

Figure 4. Calculated geometries of BODIPY-TZ compounds **3**, **4a**, **4b** and **4c** (from left to right).

The molecular orbitals are found to be localized on each subunit because electronic interactions are prevented by

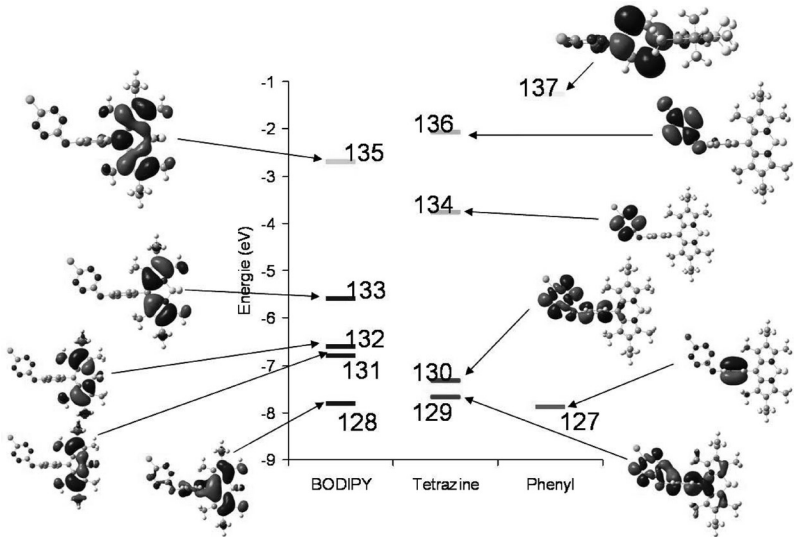

Figure 5. Energy diagram and representation of the main molecular orbitals of the various fragments in compound **4b**: LUMO (135), HOMO (133), HOMO-1 (132), HOMO-2 (131) and HOMO-5 (128) for the BODIPY core. LUMO+1 (136), LUMO (134), HOMO (130) and HOMO-1 (129) for the TZ core. LUMO (137) and HOMO (217) for the phenyl ring. As shown in the diagram, (133) and (134) correspond to the HOMO and LUMO, respectively, of compound **4b**.

their spatial arrangement (Figure 5). Indeed, sets of orbitals can be extracted that correspond to BODIPY, tetrazine and the phenyl ring. The highest occupied molecular orbital (HOMO) is always centred on the BODIPY core, which reflects its electron-donating ability. The non-bonding orbital of the tetrazine is found at a lower energy. Contrariwise, the lowest unoccupied molecular orbital (LUMO) is centred on the s-tetrazine ring and the BODIPY centred one is found at a higher energy, which corroborates the electrochemistry results. The energy gap between the HOMO and the LUMO centred on BODIPY does not change with the substitution pattern and is found to be 2.88 eV. Only in the case of **4c** is this gap smaller (2.85 eV). Such values are slightly overestimated compared with those determined from the electrochemical and spectroscopic data (2.4 eV). Nevertheless, the evolution with molecular structure agrees well with the experimental data. Indeed, the position of the absorption band does not depend upon substitution. The small red shift observed for compound **4c** compared with the others is supported by the smaller gap derived from the calculations. This is probably due to the close spatial proximity of the TZ ring. On the other hand, the energy gap between the HOMO and the LUMO centred on the tetrazine is dependent on the nature of the phenyl ring. Indeed, in the case of **3**, the presence of an additional methoxy substituent increases the energy of the LUMO by approximately 0.1 eV because of the more electron-donating nature of the phenyl ring. Hence the BODIPY ring is less affected by a change in the position of the substituents than TZ, which is confirmed by the oxidation potential (and to a lesser extent by its reduction potential) of BODIPY remaining constant whereas the reduction potential of TZ changes from –0.71 V for **4b** to –0.81 V for **3**. These results are consistent with the calculated changes in the various MO energies.

TD-DFT was also implemented to calculate the wavelengths associated with the electronic transitions in the various compounds (Table 4). The results for **3**–**5** reveal the presence of a first transition localized on the tetrazine ring at around 550 nm but its calculated oscillator strength is very small (0.002–0.004). A second intense transition is found at around 440–445 nm (f = 0.44–0.47) and is localized on the BODIPY. Thus, reconstructed spectra only show the BODIPY-centred band, which completely overshadows that of the tetrazine. This is in agreement with the experimental UV/Vis results.

Table 4. Calculated absorption wavelengths and oscillator strengths (f) using TD-DFT for all investigated compounds **1**–**5**.

Compound	λ_{abs} [nm] gaseous (solvated)	f
1a	437 (450)	0.48
1b	437 (450)	0.49
1c	439 (452)	0.49
2	437 (453)	0.47
3	439 (452)	0.47
4a	440 (452)	0.46
4b	439 (452)	0.47
4c	443 (455)	0.44
5a	431 (n.d.)	0.88
5b	431 (n.d.)	0.90

UV/Vis Spectroelectrochemistry

The evolution of the spectroscopic features of a bichromophoric BODIPY-tetrazine compound upon electrochemical reduction was investigated and compared with those of the corresponding individual chromophores. As shown in Figure 6, the UV/Vis spectrum of the bichromophore **4b** is largely similar to that of the individual chromophore **1b** as a result of the much higher absorption coefficient of the BODIPY chromophore compared with TZ. Nevertheless,

the spectroelectrochemical behaviour upon electrochemical reduction is different. Compound **1b** exhibits no variation in absorption in the wavelength range explored, whereas **4b** displays an increase in absorbance in the 550–650 nm range. This variation can be ascribed to the absorption of the anion radical of the TZ moiety, as chloromethoxy-*s*-tetrazine shows the same behaviour under similar conditions (see Figure 7). In this latter case, the appearance of new bands in the 550–650 nm and near-UV ranges is correlated to the decrease of the main absorption band, as evidenced by the isosbestic points at around 470 and 550 nm. It is thus likely that the new growing bands are actually related

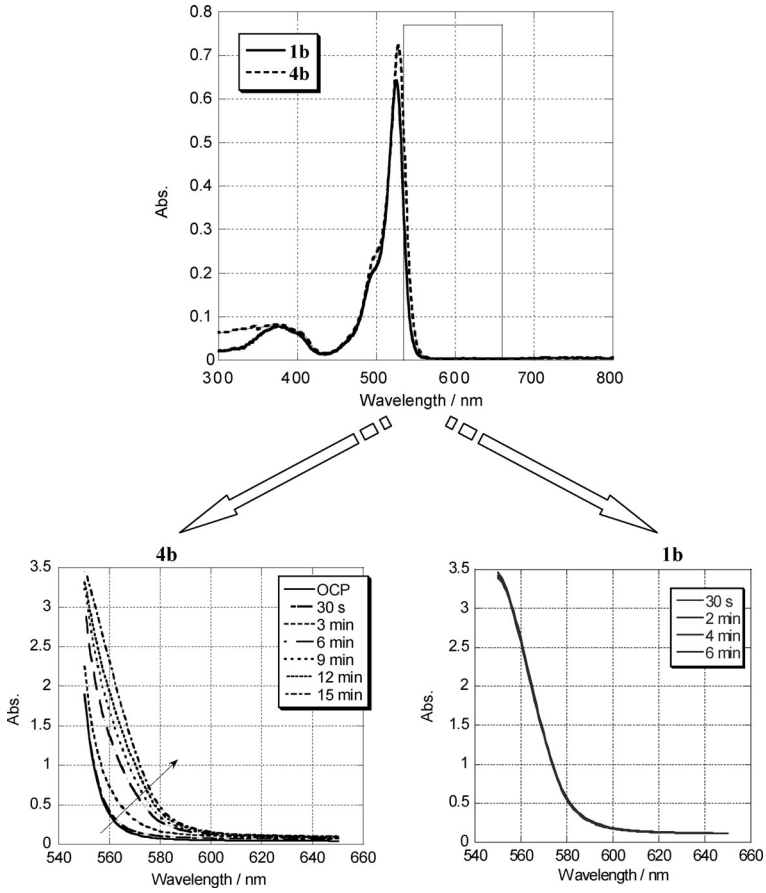

Figure 6. Spectroelectrochemical analysis of compounds **1b** and **4b** in dichloromethane. Top: at open circuit potential (OCP); bottom: at –1.2 V for the various electrolysis times displayed.

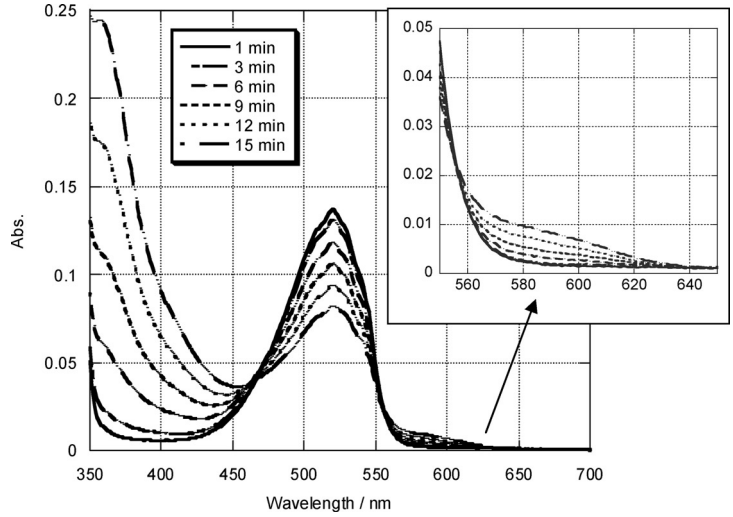

Figure 7. Spectroelectrochemical analysis of chloromethoxy-*s*-tetrazine under the same conditions as Figure 6. Inset: magnification of the 550–650 nm range.

to the electrogenerated anion radical of TZ and not to by-products (e.g., formed by the counter-electrode reaction). Further evidence for this rationale comes from the lack of variation in the absorbance of compound **1b**, which is consistent with the fact that the applied potential is not negative enough to allow electrochemical reduction of the BODIPY unit (see Table 2). A consequence of this behaviour is an overlap between the emission band of BODIPY and the absorption band of the anion radical of TZ. Hence, quenching by energy transfer is likely to occur when reducing the TZ in addition to PET from $TZ^{\bullet-}$ to the excited BODIPY. These two processes could explain the impossibility of switching on the luminescence of the bifluorophoric compounds upon reduction of TZ, as evidenced by epifluorescence microscopy coupled to electrochemistry experiments.[21]

Conclusions

Multichromophoric BODIPY-tetrazine derivatives have been synthesized and their photophysical and electrochemical properties investigated. It appears that both chromophores behave almost independently from the spectroscopic and electrochemical points of view. This result is supported by theoretical calculations that show the absence of conjugation through the phenyl ring for geometrical reasons. The absorption properties are dominated by those of BODIPY, which is thus the main emitting species. As expected the bifluorophoric derivatives exhibit very low emission quantum yields, most probably because of energy transfer rather than PET between the excited BODIPY core and the TZ moiety. Upon reduction of TZ, the system remains non-fluorescent due to both PET and a possible energy transfer from the TZ anion radical to the excited BODIPY, as evidenced by absorption spectroelectrochemistry. A detailed survey is in progress to elucidate the quenching mechanisms because interactions between the two chromophores seem to lead to rather complex behaviour.

Experimental Section

General: All solvents were dried on an automatic M. Braun SPS-800 instrument. All compounds were characterized by the usual analytical methods: ^{1}H, ^{13}C, ^{19}F and ^{10}B NMR spectra were recorded with either a Bruker Avance (300 MHz) or a JEOL ECS (400 MHz) spectrometer. All chemical shifts are referenced to Me_4Si (J values are given in Hz). Melting points were measured with a Kofler melting-point apparatus. IR spectra were measured with a Nicolet Avatar 330 FT-IR spectrometer. Mass spectra were measured at the CNRS Imagif platform (Waters spectrometer).

Synthesis of BODIPY (Procedure A): A few drops of trifluoroacetic acid were added to a dichloromethane solution of cryptopyrrole (2 equiv.) and aldehyde (1 equiv.). The dark reaction mixture was stirred at room temperature until total disappearance of the aldehyde. The oxidising agent (DDQ or chloranil, 1 equiv.), then 5 min later DIPEA (7 equiv.) and finally trifluoroborate etherate (11 equiv.) were successively added. The mixture was filtered through a pad of silica or used crude. The filtrate was concentrated and the residue purified by chromatography on silica or alumina gel or by automatic chromatography to afford BODIPY.

Synthesis of BODIPY-TZ Derivatives (Procedure B): A dry solution of BODIPY (1 equiv.) and dichloro-*s*-tetrazine (Cl_2Tz; 1 equiv.) was stirred and then 2,4,6-collidine (1 equiv.) was added. The mixture was allowed to stand either under atmospheric pressure or under a higher pressure (in a sealed tube) until no more evolution. The crude product was purified on silica gel to afford the bifluorophoric derivatives.

2,6-Diethyl-4,4-difluoro-8-(*m*-hydroxyphenyl)-1,3,5,7-dimethyl-4-bora-3a,4a-diaza-*s*-indacene (1a): The reaction was carried out using procedure A starting with cryptopyrrole (1500 mg) and 3-hydroxybenzaldehyde (750 mg). Purification on silica gel (CH_2Cl_2) afforded 940 mg of **1a** (yield 38%). ^{1}H NMR (400 MHz, $CDCl_3$): δ = 7.34 (dd, J = 8.2, J = 7.8 Hz, 1 H_{ar}), 6.93 (ddd, J = 8.2, J = 2.8, J = 0.9 Hz, 1 H_{ar}), 6.86 (ddd, J = 7.3, J = 2.3, J = 0.9 Hz, 1 H_{ar}), 6.77 (dd, J = 2.8, J = 1.4 Hz, 1 H_{ar}), 5.01 (br. s, 1 H, OH) 2.53 (s, 6 H, CH_3), 2.30 (q, J = 7.8 Hz, 4 H, CH_2-CH_3), 1.37 (s, 6 H, CH_3), 0.98 (t, J = 7.8 Hz, 6 H, CH_2CH_3) ppm. ^{13}C NMR (100 MHz, $CDCl_3$): δ = 156.6, 153.5, 139.8, 138.6, 136.8, 134.0, 133.0 (C_{ar}), 132.8, 120.2 (C_{ar}), 115.6 (C_{ar}), 115.1 (C_{ar}), 16.9, 14.4, 12.5 11.4 ppm. ^{19}F NMR (376 MHz, $CDCl_3$): δ = –145.6 (q, $J_{F\text{-}B}$ = 32.3 Hz) ppm. ^{11}B NMR (128 MHz, $CDCl_3$): δ = –0.17 (t, J = 33.2 Hz) ppm. HRMS: calcd. for $C_{23}H_{27}BF_2N_2O$ $[M + Na]^+$ 419.2082; found 419.2097.

2,6-Diethyl-4,4-difluoro-8-(*p*-hydroxyphenyl)-1,3,5,7-dimethyl-4-bora-3a,4a-diaza-*s*-indacene (1b): The reaction was carried out using procedure A starting with cryptopyrrole (1.0 g) and 4-hydroxybenzaldehyde (500 mg). Purification on silica gel (CH_2Cl_2) afforded 900 mg of **1b** (yield 56%); m.p. >290 °C. ^{1}H NMR (400 MHz, $CDCl_3$): δ = 7.12 (d, J = 8.24 Hz, 2 H_{ar}), 6.95 (d, J = 8.24 Hz, 2 H_{ar}), 2.53 (s, 6 H, CH_3), 2.31 (q, J = 7.5 Hz, 4 H, CH_2CH_3), 1.35 (s, 6 H, CH_3), 0.98 (t, J = 7.5 Hz, 6 H, CH_2CH_3) ppm. ^{13}C NMR (100 MHz, $CDCl_3$): δ = 156.48, 153.79, 140.54, 138.64, 132.97, 131.39, 129.93 (C_{ar}), 128.17, 116.29 (C_{ar}), 17.35, 14.90, 12.76, 12.12 ppm. ^{19}F NMR (376 MHz, $CDCl_3$): δ = –145.68 (q, J = 32 Hz, BF_2) ppm. ^{11}B NMR (128 MHz, $CDCl_3$): δ = –0.13 (t, J = 32 Hz) ppm. IR: $\tilde{\nu}$ = 3473 (OH), 2961, 2926, 2864 (C–H), 1614, 1537, 1474 (C=C, C=N), 1436, 1402, 1370, 1312, 1278, 1266, 1216, 1186 (B–F), 1160, 1114, 1090, 1058 (C–O), 965, 948, 918, 867, 831, 813, 799, 759, 698, 662 cm^{-1}. HRMS: calcd. for $C_{23}H_{27}BF_2N_2O$ $[M + Na]^+$ 419.2082; found 419.2097.

2,6-Diethyl-4,4-difluoro-8-(*o*-hydroxyphenyl)-1,3,5,7-dimethyl-4-bora-3a,4a-diaza-*s*-indacene (1c): The reaction was carried out using procedure A starting with cryptopyrrole (1.0 g) and salicylaldehyde (500 mg). Purification on silica gel (CH_2Cl_2/petroleum ether, 65:35) afforded 870 mg of **1c** (yield 54%); m.p. – (dec.). ^{1}H NMR (400 MHz, $CDCl_3$): δ = 7.38 (s, 1 H_{ar}), 7.30 (ddd, J = 7.50, J = 1.65 Hz, 1 H_{ar}), 7.06 (dd, J_a = 7.79, J_b = 2 Hz, 1 H_{ar}), 6.95 (m, 2 H, H_{ar}, OH), 2.48 (s, 6 H, CH_3), 2.29 (q, J = 7.5 Hz, 4 H, CH_2CH_3), 1.42 (s, 6 H, CH_3), 0.96 (t, J = 7.5 Hz, 6 H, CH_2CH_3) ppm. ^{13}C NMR (100 MHz, $CDCl_3$): δ = 153.81, 153.70, 138.44, 136.42, 132.64, 131.24 (C_{ar}), 130.72, 129.71 (C_{ar}), 122.45, 121.02 (C_{ar}), 116.75 (C_{ar}), 17.17, 14.77, 12.47, 11.01 ppm. ^{19}F NMR (376 MHz, $CDCl_3$): δ = –147 (dq, $J_{F\text{-}F}$ = 148.8, $J_{B\text{-}F1}$ = 32, $J_{B\text{-}F2}$ = 33.23 Hz) ppm. ^{11}B NMR (128 MHz, $CDCl_3$): δ = –0.37 (t, J = 33.22 Hz) ppm. IR: $\tilde{\nu}$ = 3488 (OH), 2964, 2928, 2870, 1533, 1474 (C=C, C=N), 1448, 1403, 1388, 1376, 1368, 1312, 1287, 1273, 1260, 1183 (B–F), 1160, 1115, 1104, 1056, 963, 869, 831, 800, 760, 710, 659 cm^{-1}. HRMS: calcd. for $C_{23}H_{27}BF_2N_2O$ $[M]^+$ 396.2165; found 396.2179.

2,6-Diethyl-4,4-difluoro-8-(*m*-hydroxy-*p*-methoxyphenyl)-1,3,5,7-dimethyl-4-bora-3a,4a-diaza-*s*-indacene (2): The reaction was carried out using procedure A starting with cryptopyrrole (750 mg) and 3-hydroxy-4-methoxybenzaldehyde (460 mg). Purification on silica gel (CH_2Cl_2) afforded 450 mg of **2** (yield 35%). ^{1}H NMR (400 MHz, $CDCl_3$): δ = 6.92 (d, J = 8.2 Hz, 1 H, H_{ar}), 6.82 (d, J = 1.8 Hz, 1 H, H_{ar}), 6.73 (dd, J = 8.2, J = 1.8 Hz, 1 H, H_{ar}), 3.95 (s, 3 H, O-CH_3), 2.50 (s, 6 H, CH_3), 2.29 (q, J = 7.4 Hz, 4 H, CH_2CH_3), 1.37 (s, 6 H, CH_3), 0.96 (t, J = 7.4 Hz, 6 H, CH_2CH_3) ppm. ^{13}C NMR (100 MHz, $CDCl_3$): δ = 153.56, 146.99, 146.37, 140.03, 138.55, 132.68, 131.09, 128.70, 120.16, 114.82, 111.03, 56.05, 17.16, 14.73, 12.57, 11.84 ppm. IR: $\tilde{\nu}$ = 2967, 2923, 1540, 1476, 1405, 1190, 1066, 1057, 978, 756 cm^{-1}. HRMS: calcd. for $C_{24}H_{29}BF_2N_2O_2$ $[M + Na]^+$ 449.2188; found 449.2190.

8-[*m*-(*p*-Chloro-*s*-tetrazinyloxy)-*p*-methoxyphenyl]-2,6-diethyl-4,4-difluoro-1,3,5,7-dimethyl-4-bora-3a,4a-diaza-*s*-indacene (3): The reaction was carried out using procedure B starting with **2** (285 mg) and $TzCl_2$ (100 mg, 1 equiv.) Purification by chromatography on silica gel (CH_2Cl_2/petroleum ether, 6:4) afforded 200 mg of **3** (yield 55%); m.p. – (dec.). ^{1}H NMR (300 MHz, $CDCl_3$): δ = 7.10 (m, 3 H, H_{ar}), 3.68 (s, 3 H, O-CH_3), 2.72 (s, 6 H, CH_3), 2.14 (m, 4 H, CH_2CH_3), 1.28 (s, 6 H, CH_3), 0.81 (m, 6 H, CH_2CH_3) ppm. ^{13}C NMR (75 MHz, $CDCl_3$): δ = 167.71, 165.29, 153.98, 152.64, 141.02, 138.37, 137.94, 133.01, 130.86, 127.96 (C_{ar}), 125.39 (C_{ar}), 122.22 (C_{ar}), 113.46 (C_{ar}), 56.15, 17.00, 14.62, 12.47, 12.06 ppm. IR: $\tilde{\nu}$ = 2969, 2900, 1542, 1476, 1441, 1354, 1321, 1191, 1066, 979 cm^{-1}. HRMS: calcd. for $C_{26}H_{28}BClF_2N_6O_2$ $[M + Na]^+$ 563.1921; found 563.1931.

8-[*m*-(*p*-Chloro-*s*-tetrazinyloxy)phenyl]-2,6-diethyl-4,4-difluoro-1,3,5,7-dimethyl-4-bora-3a,4a-diaza-*s*-indacene (4a): The reaction was carried out using procedure B starting with **1a** (400 mg) and $TzCl_2$ (150 mg, 1 equiv.). Purification by chromatography on silica gel (CH_2Cl_2/petroleum ether, 95:5) afforded 200 mg of **4a** (yield 39%) and 130 mg of **5a** (15%); m.p. – (dec.). ^{1}H NMR (300 MHz, $CDCl_3$): δ = 7.67 (dd, J = 8.1, J = 7.4 Hz, 1 H, H_{ar}), 7.43 (d, J = 8.1 Hz, 1 H, H_{ar}), 7.36 (d, J = 7.4 Hz, 1 H, H_{ar}), 7.28 (s, 1 H, H_{ar}), 2.53 (s, 6 H, CH_3), 2.33 (q, J = 7.5 Hz, 4 H, CH_2CH_3), 1.45 (s, 6 H, CH_3), 1.01 (t, J = 7.5 Hz, CH_2CH_3) ppm. ^{13}C NMR (75 MHz, $CDCl_3$): δ = 167.57, 165.35, 154.31, 152.32, 138.15, 138.10, 137.43, 133.07, 131.08, 130.33, 127.08, 121.25, 121.20, 16.96, 14.51, 12.43, 11.77 ppm. HRMS: calcd. for $C_{25}H_{26}BF_2N_6O$ $[M + Na]^+$ 533.1815; found 533.1827.

8-[*p*-(*p*-Chloro-*s*-tetrazinyloxy)phenyl]-2,6-diethyl-4,4-difluoro-1,3,5,7-dimethyl-4-bora-3a,4a-diaza-*s*-indacene (4b): The reaction was carried out using procedure B starting with **1b** (200 mg) and $TzCl_2$ (76 mg). Purification by chromatography on silica gel (CH_2Cl_2/petroleum ether, 5:5) afforded 92 mg of **4b** (yield 36%); m.p. – (dec.). ^{1}H NMR (400 MHz, $CDCl_3$): δ = 7.44 (m, 4 H, H_{ar}), 2.53 (s, 6 H, CH_3), 2.32 (q, J = 7.5 Hz, 4 H, CH_2CH_3), 1.38 (s, 6 H, CH_3), 0.99 (t, J = 7.5 Hz, CH_2CH_3) ppm. ^{13}C NMR (100 MHz, $CDCl_3$): δ = 167.55, 165.45, 154.24, 152.09, 138.31, 138.21, 134.67, 133.14, 130.68, 130.40 (C_{ar}), 121.73 (C_{ar}), 17.08, 14.63, 12.54, 11.95 ppm. ^{19}F NMR (376 MHz, $CDCl_3$): δ = –145.61 (q, $J_{F\text{-}B}$ = 33 Hz) ppm. ^{11}B NMR (128 MHz, $CDCl_3$): δ = –0.21 (t, $J_{B\text{-}F}$ = 33 Hz) ppm. IR: $\tilde{\nu}$ = 2968, 2928, 2870 (C–H), 1536, 1474 (C=C, C=N), 1434, 1389, 1371, 1353, 1319, 1273, 1186 (B–F), 1114, 1157, 1080 (C–Cl), 1059 (C–O), 1034, 1019, 972, 933, 890, 851, 817, 802, 763, 720, 694, 661 cm^{-1}. HRMS: calcd. for $C_{25}H_{26}BF_2N_6O$ $[M + Na]^+$ 533.1815; found 533.1826.

8-[*o*-(*p*-Chloro-*s*-tetrazinyloxy)phenyl]-2,6-diethyl-4,4-difluoro-1,3,5,7-dimethyl-4-bora-3a,4a-diaza-*s*-indacene (4c): The reaction was carried out using procedure B starting with **1b** (600 mg) and $TzCl_2$ (113 mg) in a sealed tube at 125 °C. Purification by chromatography on silica gel (CH_2Cl_2/petroleum ether, 5:5) afforded 145 mg of **4c** (yield 37%); m.p. – (dec.). ^{1}H NMR (400 MHz, $CDCl_3$): δ = 7.91 (ddd, J_g = 8.24, J_m = 7.33, ^4J = 1.83 Hz, 1 H, H_{ar}), 7.78 (ddd, J_g = 7.79, J_m = 7.33, ^4J = 0.92 Hz, 1 H, H_{ar}), 7.73 (dd, J_g = 7.33, ^4J = 1.83 Hz, 1 H, H_{ar}), 7.68 (dd, J_g = 8.24, ^4J = 0.92 Hz, 1 H, H_{ar}), 2.78 (s, 6 H, CH_3), 2.59 (q, J = 7.5 Hz, 4 H, CH_2CH_3), 1.78 (s, 6 H, CH_3), 1.28 (t, J = 7.5 Hz, 6 H, CH_2CH_3) ppm. ^{13}C NMR (100 MHz, $CDCl_3$): δ = 167.40, 165.35, 154.87, 150.17, 138.23, 133.36, 132.79, 130.62, 131.40, 131.10, 128.33, 127.42, 122.39, 17.41, 14.86, 12.88, 11.80 ppm. ^{19}F NMR (376 MHz, $CDCl_3$): δ = –145.6 (large multiplet) ppm. ^{11}B NMR (128 MHz, $CDCl_3$): δ = –0.40 (t, J = 33 Hz) ppm. IR: $\tilde{\nu}$ = 2966, 2928, 2871 (C–H), 1535, 1473 (C=C, C=N), 1434, 1404, 1389, 1371, 1352, 1319, 1272, 1186 (B–F), 1157, 1114, 1080 (C–Cl), 1059, 1035, 1019, 972, 933, 890, 852, 817, 764, 720, 695, 659 cm^{-1}. HRMS: calcd. for $C_{25}H_{26}BClF_2N_6O$ $[M]^+$ 510.1898; found 510.1912.

2,6-Diethyl-4,4-difluoro-1,3,5,7-dimethyl-8-[*o*-phenyloxy-*p*-(*p*PCB)-*s*-tetrazine]-4-bora-3a,4a-diaza-*s*-indacene (5a): Compound **5a** was prepared along with **4a** in the reaction described above to give 200 mg of **4a** (yield 39%) and 130 mg of **5a** (15%); m.p. – (dec.). ^{1}H NMR (300 MHz, $CDCl_3$): δ = 7.64 (dd, J = 7.7, J = 8.0 Hz, 2 H, H_{ar}), 7.42 (dd, J = 7.8, J = 2.0 Hz, 2 H, H_{ar}), 7.32 (d, J = 8.0 Hz, 2 H, H_{ar}), 7.25 (s, 2 H, H_{ar}), 2.56 (s, 12 H, CH_3) 2.34 (q, J = 7.3 Hz, 8 H, CH_2CH_3), 1.43 (s, 12 H, CH_3), 1.02 (t, J = 7.3 Hz, 12 H, CH_2CH_3) ppm. ^{13}C NMR (75 MHz, $CDCl_3$): δ = 167.35, 154.24, 153.01, 138.18, 137.87, 137.69, 132.99, 130.94, 130.37, 126.52, 121.17 (C_{ar}), 121.16 (C_{ar}), 16.98, 14.40, 12.35, 11.64 ppm. IR: $\tilde{\nu}$ = 2969, 2901, 1541, 1475, 1406, 1382, 1320, 1190, 1066, 979 cm^{-1}. HRMS: calcd. for $C_{48}H_{52}B_2F_4N_8O_2$ $[M + Na]^+$ 893.4233; found 893.4258.

2,6-Diethyl-4,4-difluoro-1,3,5,7-dimethyl-8-[*o*-phenyloxy-*p*-(*p*PCB)-*s*-tetrazine]-4-bora-3a,4a-diaza-*s*-indacene (5b): The reaction was carried out using procedure B starting with **2** (630 mg) and $TzCl_2$ (90 mg) in a sealed tube at 125 °C. Purification by chromatography on alumina gel (CH_2Cl_2/petroleum ether, 5:5) afforded 92 mg of **5b** (yield 18%); m.p. – (dec.). ^{1}H NMR (400 MHz, $CDCl_3$): δ = 7.12 (d, J = 7.79 Hz, 4 H, H_{ar}), 6.94 (d, J = 7.79 Hz, 4 H, H_{ar}), 2.54 (s, 12 H, CH_3), 2.32 (q, J = 7.33 Hz, 8 H, CH_2CH_3), 1.38 (s, 12 H, CH_3), 0.99 (t, J = 7.30 Hz, 12 H, CH_2CH_3) ppm. ^{13}C NMR (100 MHz, $CDCl_3$): δ = 167.54, 154.47, 153.09, 138.79, 138.48, 134.40, 133.36, 131.00, 130.54 (C_{ar}), 121.82 (C_{ar}), 27.93, 22.86, 15.52, 14.86 ppm. ^{19}F NMR (376 MHz, $CDCl_3$): δ = –145.64 (q, J = 33 Hz) ppm. ^{11}B NMR (128 MHz, $CDCl_3$): δ = –15 (t, J = 33 Hz) ppm. IR: $\tilde{\nu}$ = 2965, 2925, 2870 (C–H), 1540, 1474 (C=C, C=N), 1404, 1373, 1318, 1262, 1187 (B–F), 1115, 1063 (C–O), 1019, 978, 924, 885, 849, 808, 783, 758, 734, 701 cm^{-1}. MS (TOF ES+): calcd. for $[C_{48}H_{52}B_2F_4N_8O_2 + Na]^{+\cdot}$ 893.4233; found 893.425.

Photophysical Measurements: The solvents used were purchased from Sigma–Aldrich and were all of spectroscopic grade. Excitation and emission spectra were measured with a SPEX Fluorolog-3 (Jobin–Yvon) spectrometer. A right-angle configuration was used and the optical density was adjusted to below 0.1 to avoid reabsorption artefacts. Fluorescence decay curves in solution were obtained using a time-correlated single-photon counting method using a titanium-sapphire laser pumped by an argon ion laser (Tsunami, by Spectra-Physics, 82 MHz, 1 ps pulse width, repetition rate lowered to 4 MHz with a pulse-peaker, a doubling crystal was used to reach 495 nm excitation). The Levenberg–Marquardt algorithm was used for the non-linear least-squares fit.

Electrochemistry and Absorption Spectroscopy: Solvents (SDS, HPLC grade) and electrolyte salts (tetrabutylammonium hexafluo-

rophosphate from Fluka, puriss.) were used without further purification. Cyclic voltammetry was performed in a three-electrode cell with a potentiostat (CH Instruments 600) driven by a PC. Platinum or gold disk electrodes (1 mm diameter) were used as working electrodes, whereas platinum wire and Ag^+ (0.01 M in acetonitrile)/Ag were used, respectively, as the counter and reference electrodes. All the investigated solutions were deaerated by argon-bubbling for at least 5 min before performing the electrochemical measurements.

Absorption spectra were recorded with a Cary 500 (Varian) spectrophotometer in 1 cm optical length quartz cuvettes. Absorption spectroelectrochemistry was performed in the same cuvette using an ITO plate as the working electrode, a Mg wire as a sacrificial anodic counter-electrode and an Ag wire as a pseudo-reference electrode.

Quantum Chemical Calculations: Calculations were performed with the Gaussian 03 software[22] at the MESO calculation centre of the ENS Cachan (Nec TX7 with 32 processors of type Itanium 2). All calculations were performed at the B3LYP/6-31+G(d) of theory.

Supporting Information (see also the footnote on the first page of this article): **S1**: CV of compound **5b** in dichloromethane (scan rate: 100 mV/s). **S2**: Spin density from B3LYP calculations performed on the cation radical, anion radical and dianion of **4b**.

[1] a) L. Flamigni, J. P. Collin, J. P. Sauvage, *Acc. Chem. Res.* **2008**, *41*, 857; b) A. Sautter, B. K. Kaletas, D. G. Schmid, R. Dobrawa, M. Zimine, G. Jung, I. H. M. Van Stokkum, L. De Cola, R. M. Williams, F. Wurthner, *J. Am. Chem. Soc.* **2005**, *127*, 6719; c) J. Baffreau, S. Leroy-Lhez, N. Van Anh, R. M. Williams, P. Hudhomme, *Chem. Eur. J.* **2008**, *14*, 4974; d) J. Baffreau, S. Leroy-Lhez, P. Hudhomme, M. M. Groeneveld, I. H. M. Van Stokkum, R. M. Williams, *J. Phys. Chem. A* **2006**, *110*, 13123; e) F. Würtner, *Chem. Commun.* **2004**, 1564.

[2] a) A. P. De Silva, N. H. Q. Gunaratne, T. Gunnlaugsson, A. J. M. Huxley, C. P. McCoy, J. T. Rademacher, T. E. Rice, *Chem. Rev.* **1997**, *97*, 1515; b) B. K. Kaleta, R. M. Williams, B. König, L. De Cola, *Chem. Commun.* **2002**, 776; c) A. P. De Silva, N. H. Q. Gunaratne, C. P. McCoy, *Nature* **1993**, *364*, 42.

[3] a) W. G. J. H. M. Van Sark, K. W. J. Barnham, L. H. Slooff, A. J. Chatten, A. Buchtemann, A. Meyer, S. J. McCormack, R. Koole, D. J. Farrell, R. Bose, E. E. Bende, A. R. Burgers, T. Budel, J. Quilitz, M. Kennedy, T. Meyer, C. D. M. Donega, A. Meijerink, D. Vanmaekelbergh, *Optics Express* **2008**, *16*, 21773; b) M. J. Currie, J. K. Mapel, T. D. Heidel, S. Goffri, M. A. Baldo, *Science* **2008**, *321*, 226.

[4] a) R. L. Zhang, Z. L. Wang, Y. S. Wu, H. B. Fu, J. N. Yao, *Org. Lett.* **2008**, *10*, 3065; b) T. Suzuki, A. Migita, H. Higushi, H. Kawai, T. Fujiwara, K. Tsuji, *Tetrahedron Lett.* **2003**, *44*, 6837; c) A. C. Benniston, G. Copley, K. J. Elliot, R. W. Harrington, W. Clegg, *Eur. J. Org. Chem.* **2008**, 2705; d) S. Leroy-Lhez, L. Perrin, J. Baffreau, P. Hudhomme, *C. R. Chim.* **2006**, *9*, 240.

[5] a) H. Oevering, M. N. Paddon-Row, M. Heppener, A. M. E. Oliver, E. Cotsaris, J. W. Verhoeven, N. S. Hush, *J. Am. Chem. Soc.* **1987**, *109*, 3258; b) R. M. Williams, J. M. Zwier, J. W. Verhoeven, *J. Am. Chem. Soc.* **1995**, *117*, 4093; c) M. T. Indelli, C. Chiorboli, F. Flamigni, L. De Cola, F. Scandola, *Inorg. Chem.* **2007**, *46*, 5630; d) T. Nakamura, J. Ikemoto, M. Fujitsuka, Y. Araki, O. Ito, K. Takimiya, Y. Aso, T. Otsubo, *J. Phys. Chem. B* **2005**, *109*, 14365.

[6] a) Y. Kim, E. Kim, G. Clavier, P. Audebert, *Chem. Commun.* **2006**, 3612; b) F. Miomandre, R. Meallet-Renault, J. J. Vachon, R. B. Pansu, P. Audebert, *Chem. Commun.* **2008**, 1913.

[7] P. Audebert, F. Miomandre, G. Clavier, M. C. Vernières, S. Badré, R. Méallet-Renault, *Chem. Eur. J.* **2005**, *11*, 5667.

[8] a) A. Loudet, K. Burgess, *Chem. Rev.* **2007**, *107*, 4891; b) T. E. Wood, A. Thompson, *Chem. Rev.* **2007**, *107*, 1831.

[9] a) I. J. Arroyo, R. Hu, G. Merino, B. Zhong Tang, E. Pea-Cabrera, *J. Org. Chem.* **2009**, *74*, 5719; b) A. Schmitt, B. Hinkeldey, M. Wild, G. Jung, *J. Fluoresc.* **2009**, *19*, 755; c) K. Trama, H. Yana, H. A. Jenkins, S. Vassiliev, D. Bruce, *Dyes Pigm.* **2009**, *82*, 392.

[10] a) J. Karolin, L. B.-A. Johansson, L. Strandberg, T. Ny, *J. Am. Chem. Soc.* **1994**, *116*, 7801; b) R. P. Haugland, *Handbook of Fluorescent Probes and Research Chemicals*, 6th ed., Molecular Probes, Eugene, OR, **1996**; c) K. Tan, L. Jaquinod, R. Paolesse, S. Nardis, C. Di Natale, A. Di Carlo, L. Prodi, M. Montalti, N. Zaccheroni, K. M. Smith, *Tetrahedron* **2004**, *60*, 1099; d) M.-c. Yee, S. C. Fas, M. M. Stohlmeyer, T. J. Wandless, K. A. Cimprich, *J. Biol. Chem.* **2005**, *280*, 29053; e) R. W. Wagner, J. S. Lindsey, *Pure Appl. Chem.* **1996**, *68*, 1373.

[11] M. L. Metzker, WO Patent WO/2003/066812, **2003**.

[12] a) T. A. Golovkova, D. V. Kozlov, D. C. Neckers, *J. Org. Chem.* **2005**, *70*, 5545; b) C. Trieflinger, K. Rurack, J. Daub, *Angew. Chem. Int. Ed.* **2005**, *44*, 2288; c) H. Rohr, C. Trieflinger, K. Rurack, J. Daub, *Chem. Eur. J.* **2006**, *12*, 689; d) A. Ambroise, R. W. Wagner, P. D. Rao, J. A. Riggs, P. Hascoat, J. R. Diers, J. Seth, R. K. Lammi, D. F. Bocian, D. Holten, J. S. Lindsey, *Chem. Mater.* **2001**, *13*, 1023; e) G. Beer, C. Niederalt, S. Grimme, J. Daub, *Angew. Chem. Int. Ed.* **2000**, *39*, 3252.

[13] a) K. Yamada, Y. Nomura, D. Citterio, N. Iwasawa, K. Suzuki, *J. Am. Chem. Soc.* **2005**, *127*, 6956; b) J. D. Blakemore, R. Chitta, F. D'Souza, *Tetrahedron Lett.* **2007**, *48*, 1977.

[14] a) M. Álvarez, A. Costela, I. García-Moreno, F. Amat-Guerri, M. Liras, R. Sastre, F. López Arbeloa, J. Bañuelos Prieto, I. López Arbeloa, *Photochem. Photobiol. Sci.* **2008**, *7*, 802; b) A. Costela, I. Garcia-Moreno, *J. Photochem. Photobiol. A: Chem.* **2008**, *198*, 192; c) I. García-Moreno, F. Amat-Guerri, M. Liras, A. Costela, L. Infantes, R. Sastre, F. López Arbeloa, J. Bañuelos Prieto, Í. López Arbeloa, *Adv. Funct. Mater.* **2007**, *17*, 3088.

[15] T. Rousseau, A. Cravino, T. Bura, G. Ulrich, R. Ziessel, J. Roncali, *Chem. Commun.* **2009**, 1673.

[16] a) R. Ziessel, B. D. Allen, D. B. Rewinska, A. Harriman, *Chem. Eur. J.* **2009**, *15*, 7382; b) S. Hattori, K. Ohkubo, Y. Urano, H. Sunahara, T. Nagano, Y. Wada, N. V. Tkachenko, H. Lemmetyinen, S. Fukuzumi, *J. Phys. Chem. B* **2005**, *109*, 15368; c) A. C. Benniston, G. Copley, A. Harriman, D. B. Rewinska, R. W. Harrington, W. Clegg, *J. Am. Chem. Soc.* **2008**, *130*, 7174; d) M. Galleta, F. Puntoriero, S. Campagna, C. Chiorbolli, M. Quesada, S. Goeb, R. Ziessel, *J. Phys. Chem. A* **2006**, *110*, 4348.

[17] a) M. Broring, R. Kruger, S. Link, C. Kleeberg, S. Kohler, X. Xie, B. Ventura, L. Flamigni, *Chem. Eur. J.* **2008**, *14*, 2976; b) Y. Cakmak, E. U. Akkaya, *Org. Lett.* **2009**, *11*, 85.

[18] J. Banuelos, F. Lopez Arbeola, T. Arbeloa, S. Salleres, F. Amat-Guerri, M. Liras, I. Lopez Arbeaola, *J. Phys. Chem. A* **2008**, *112*, 10816.

[19] D. E. Chavez, R. D. Gilardi, M. A. Hiskey, *Angew. Chem. Int. Ed.* **2000**, *39*, 1791.

[20] T. Matsumoto, Y. Urano, T. Shoda, H. Kojima, T. Nagano, *Org. Lett.* **2007**, *9*, 3375.

[21] F. Miomandre, E. Lépicier, O. Galangau, C. Dumas-Verdes, P. Audebert, R. Méallet-Renault, R. B. Pansu, manuscript submitted.

[22] M. J. Frisch, G. W. Trucks, H. B. Schlegel, G. E. Scuseria, M. A. Robb, J. R. Cheeseman, J. A. Montgomery Jr., T. Vreven, K. N. Kudin, J. C. Burant, J. M. Millam, S. S. Iyengar, J. Tomasi, V. Barone, B. Mennucci, M. Cossi, G. Scalmani, N. Rega, G. A. Petersson, H. Nakatsuji, M. Hada, M. Ehara, K. Toyota, R. Fukuda, J. Hasegawa, M. Ishida, T. Nakajima, Y. Honda, O. Kitao, H. Nakai, M. Klene, X. Li, J. E. Knox, H. P. Hratchian, J. B. Cross, C. Adamo, J. Jaramillo, R. Gomperts, R. E. Stratmann, O. Yazyev, A. J. Austin, R. Cammi, C. Pomelli, J. W. Ochterski, P. Y. Ayala, K. Morokuma, G. A. Voth, P.

Salvador, J. J. Dannenberg, V. G. Zakrzewski, S. Dapprich, A. D. Daniels, M. C. Strain, O. Farkas, D. K. Malick, A. D. Rabuck, K. Raghavachari, J. B. Foresman, J. V. Ortiz, Q. Cui, A. G. Baboul, S. Clifford, J. Cioslowski, B. B. Stefanov, G. Liu, A. Liashenko, P. Piskorz, I. Komaromi, R. L. Martin, D. J. Fox, T. Keith, M. A. Al-Laham, C. Y. Peng, A. Nanayakkara, M. Challacombe, P. M. W. Gill, B. Johnson, W. Chen, M. W. Wong, C. Gonzalez, J. A. Pople, *Gaussian 03*, *Revision C.02*, Gaussian Inc., Wallingford, CT, **2004**.

Received: July 31, 2009
Revision Received: January 13, 2010
Published Online: March 26, 2010

